

Mechanisms of Activation and Subunit Release in Ca²⁺/Calmodulin Dependent Protein Kinase II

Filippo Pullara, Eliana Karina Ascitutto, and Ignacio Jose General

J. Phys. Chem. B, **Just Accepted Manuscript** • DOI: 10.1021/acs.jpcc.7b09214 • Publication Date (Web): 18 Oct 2017

Downloaded from <http://pubs.acs.org> on October 20, 2017

Just Accepted

“Just Accepted” manuscripts have been peer-reviewed and accepted for publication. They are posted online prior to technical editing, formatting for publication and author proofing. The American Chemical Society provides “Just Accepted” as a free service to the research community to expedite the dissemination of scientific material as soon as possible after acceptance. “Just Accepted” manuscripts appear in full in PDF format accompanied by an HTML abstract. “Just Accepted” manuscripts have been fully peer reviewed, but should not be considered the official version of record. They are accessible to all readers and citable by the Digital Object Identifier (DOI®). “Just Accepted” is an optional service offered to authors. Therefore, the “Just Accepted” Web site may not include all articles that will be published in the journal. After a manuscript is technically edited and formatted, it will be removed from the “Just Accepted” Web site and published as an ASAP article. Note that technical editing may introduce minor changes to the manuscript text and/or graphics which could affect content, and all legal disclaimers and ethical guidelines that apply to the journal pertain. ACS cannot be held responsible for errors or consequences arising from the use of information contained in these “Just Accepted” manuscripts.



1
2
3 Mechanisms of Activation and Subunit Release in Ca²⁺/Calmodulin Dependent
4
5
6 Protein Kinase II
7
8
9

10
11 Filippo Pullara,^{1¶} Eliana K. Ascitto,^{2¶} Ignacio J. General^{2*}
12

13
14 ¶These authors contributed equally to this work
15

16
17 *Corresponding author: ijgeneral@gmail.com
18

19
20 ¹Department of Computational and Systems Biology, School of Medicine, University of Pittsburgh,
21 Pennsylvania, U.S.A.
22

23
24 ²School of Science and Technology, Universidad Nacional de San Martín, and CONICET, 25 de Mayo
25 y Francia, San Martín (1650), Buenos Aires, Argentina
26
27
28
29
30
31
32
33
34
35
36
37
38
39
40
41
42
43
44
45
46
47
48
49
50
51
52
53
54
55
56
57
58
59
60

1
2 **ABSTRACT:** Calcium/Calmodulin dependent protein kinase II is an enzyme involved in many
3
4 different functions, including the so-called long-term potentiation, a mechanism that
5
6 strengthens synapses in a persistent mode, and is believed to be a basic cellular mechanism
7
8 for memory formation. Here we study the conformational changes of the enzyme due to
9
10 phosphorylation of some key residues that are believed to drive the transition from an
11
12 inhibited to an active state; it is this active state the one associated with long-term
13
14 potentiation. We found that the conformational changes could be explained in terms of three
15
16 charged regions in the three main subdomains of the enzyme, hub, linker and kinase. The
17
18 role of phosphorylation is to change the charge relation between them, turning on and off their
19
20 interactions, switching between an attractive state (non-phosphorylated or inhibited) and a not
21
22 attractive one (phosphorylated or active). We also show that phosphorylated subunits become
23
24 less stable and this could favor their release from the multimer, as has been already observed
25
26 experimentally.
27
28
29
30
31
32
33
34
35
36
37
38
39
40
41
42
43
44
45
46
47
48
49
50
51
52
53
54
55
56
57
58
59
60

INTRODUCTION

Calcium/calmodulin dependent protein kinase II, CaMKII, is a serine/threonine specific kinase, which is regulated by the calcium/calmodulin complex. This enzyme is involved in many biological processes, such as calcium regulation¹, signal transduction in epithelia², the cell cycle³ and T-cell activation⁴. However, one of the most important aspects of CaMKII, for which it is and has been actively studied, is related to the regulation of certain neuronal processes, including long-term potentiation (LTP), i.e., the enhancement of synapses related to memory formation⁵.

There are four CaMKII genes in humans, α , β , γ and δ , which are expressed in at least 38 isoforms⁶, through alternative splicing. There is a large sequence identity between the different human isoforms, and the largest difference is found in the length of the linker connecting the C and N domains: it can have a large variation in size, and this change affects the frequency response of CaMKII to Calcium/Calmodulin pulses⁷. In this work, we study the α isoform of CaMKII, predominantly found in the brain, with a β 7 linker, which has been showed to have a reduced kinase activity⁸.

Structurally, the variant of CaMKII we study in this work is a dodecamer, composed of two rings, stacked one on top of the other, and each formed by six subunits (SUs). Each SU of the system is composed of three subdomains: C-terminal hub (H), located towards the center of the ring, forming the core of the system; linker (L) connecting H with the exterior part of the SU, the N-terminal kinase (K). These Ks are responsible for the phosphorylation of other neighboring kinases, both in the same dodecamer and in others. Their activity depends on the overall structure of the subunit. That is, a closed conformation, where K is docked onto H, does not allow the flexibility a kinase needs in order to phosphorylate its neighbors, and thus it is called an autoinhibited structure. On the other hand, an open conformation, with K moving away from H allows for an active kinase.

Hence, the activation process is thought to begin with a SU in a closed form, with its K domain

1
2 docked onto H. Ca/CaM binds around amino acids T305/306, resulting in the displacement of an
3
4 inhibitory regulatory segment, and opening of the SU (see **Fig. 1**, right panel). This is followed by
5
6 phosphorylation of T286, which inhibits re-binding of the segment to the kinase domain, thus keeping
7
8 the SU in an open conformation. Consequently, this kinase can later phosphorylate a neighboring SU in
9
10 the same dodecamer (trans-phosphorylation). Persistence of this kinase active state is thought to be
11
12 fundamental for the LTP process^{9,10}, while a quick return to an inactive state (through lack of T286
13
14 phosphorylation) would not allow such process. Rebinding of Ca/CaM to T305/306, which could
15
16 stimulate a return to the closed conformation, is prevented by the phosphorylation of either^{11,12,13}.
17
18
19
20
21 These two sites are also known to be related to LTP¹⁴.

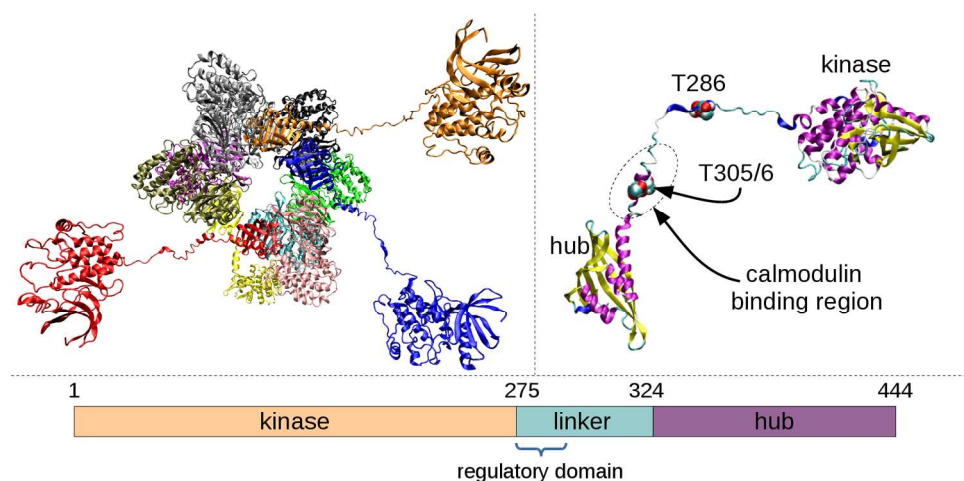


Fig. 1: Left panel) Modeled CaMKII dodecamer. It is a stack of two rings, each with six SUs, shown in different colors (one ring is behind the other, so they are not clearly distinguishable). Eight of the SUs are in their closed conformations, while another four—blue, red and orange in the front ring, and yellow in the back (mostly hidden)—were modeled in the open state. Right panel) Representation of one of the SUs, showing the hub and kinase subdomains, connected via a flexible linker, and highlighting T286, T305 and T306, phosphorylation sites known to be critical for the protein's function. Lower panel) Schematic view of the three subdomains.

The mechanism governing the process just described is not well understood at the molecular

1
2 level. Using elastic network models and molecular dynamics (MD), we show in this study the effects of
3
4 phosphorylation on the dynamics of the system, and highlight the relevance of specific regions of the
5
6 H, L and K subdomains, in determining the behavior of the protein.
7

8
9 We also inspect the stability of the system, and evaluate the experimental observation of the
10
11 spontaneous release of SUs upon activation. This release event is thought to be the way in which an
12
13 activated SU can be dropped from an already active CaMKII molecule, and later be inserted in an
14
15 inhibited one, thus kick-starting its activation via transphosphorylation of the same enzyme's
16
17 neighboring SUs.¹⁵
18
19

20 21 22 23 24 25 **METHODS** 26

27
28 The crystal structure with pdb code 3SOA¹⁶ describes human CaMKII in its α isoform, with a β 7
29
30 linker, in a closed or auto-inhibited conformation. This isoform is the one with the highest
31
32 concentration in neurons¹⁵. The 3SOA structure is the one we used to form the closed subunits of the
33
34 CaMKII dodecamer employed for our simulations. On the other hand, the 2WEL¹⁷ pdb crystal structure
35
36 contains a calmodulin-bound CaMKII in its delta isoform, in an open conformation. Since the kinase
37
38 domains of both isoforms have a high sequence similarity—about 93%—we combined the hub of
39
40 both, open and closed SUs, follows that of 3SOA, with the kinase being formed by residues 1 to 275,
41
42 and the hub by 324 to 444. Finally, combining eight closed and four open subunits, a CaMKII
43
44 dodecameric system, without calmodulin, was created, forming the initial model for our systems, as
45
46 shown in **Fig. 1**. The resulting simulation box contains, after solvation with TIP3P water¹⁸, more than
47
48 1.2 million atoms.
49
50
51
52
53
54

55
56 In order to drive the modeled molecule to a stable conformation, we ran several cycles of
57
58 minimization and equilibration. The simulations in this work were performed using the AMBER15¹⁹
59
60

1 software package, with all of them—except for the minimizations—using the GPU version of the
2 PMEMD program. We employed the Amber12 force field. The systems were kept at a temperature of
3
4 298 K, using Langevin dynamics with a collision frequency of 2 ps^{-1} , and a pressure of 1 atm, via a
5
6 weak-coupling Berendsen barostat, with a relaxation time of 2 ps. The SHAKE algorithm was adopted,
7
8 allowing the use of a 2 fs time step. The protocol followed for minimization and equilibration was: 1)
9
10 100 cycles of minimization, using AMBER's XMIN method, followed by 5,000 cycles using steepest
11
12 descent, and another 5,000 steps using conjugate gradient; 2) 1 ns of heating, to 298 K, followed by
13
14 another ns at constant T and P (1 atm), and finally 20 ns with constant T. This equilibrated structure
15
16 was then used as a starting point for the construction of the 3 different systems we studied, differing in
17
18 the phosphorylation state of residues T286, T305 and T306: 1) Non-Phosphorylated (NP) system, with
19
20 no phosphorylation of those residues, 2) Phosphorylated (P) system, with phosphorylation of T286 in
21
22 the four open subunits, and 3) All-Phosphorylated (AP) system, with the 3 mentioned residues
23
24 phosphorylated, also in the four open subunits.
25
26
27
28
29
30
31

32
33 The addition of the phosphate group was achieved by replacing the involved threonines' side
34
35 chains, by phosphorylated ones: parametrized phospho-threonines with a single protonated phosphate
36
37 group, THR-PO₂(OH), with electric charge -1 ^{20,21}, consistent with the AMBER family of force-fields.
38
39

40 Once the P and AP systems were created by adding a phosphate group to T286 and
41
42 T286,305,306, respectively, we repeated the equilibration protocol described before, for each of the
43
44 three new systems (including NP). We finally took the three last frames obtained for each system as the
45
46 initial structures for the NP, P and AP models.
47
48

49 From them, we started ~ 400 ns long conventional MD (cMD) simulations, which constitute the
50
51 three MD trajectories analyzed in this work. In addition, taking the initial 20 ns of these simulations,
52
53 we calculated the average potential and dihedral energies of each of them, and used that information to
54
55 calculate the parameters needed to start an accelerated MD (aMD) simulation²² for each system.
56
57
58

59 In summary, we ended up with 3 systems of CaMKII—NP, P and AP—all of them with four
60

open SUs and the other eight closed, and none of them contained calmodulin. For each system we ran 2 simulations, one cMD and one aMD, obtaining, in the end, a total of 6 trajectories, with an overall simulation time of about 2.4 microseconds (if we consider the acceleration of the aMD trajectories, the effective simulation time becomes much longer).

RESULTS AND DISCUSSION

The First 1% of ANM Modes Explains the Closed to Open Transition of Subunits. Elastic networks are idealized models of molecules that have been successful at explaining many dynamical aspects of proteins. In this work, we applied the Anisotropic Network Model (ANM)²³ to show how the system's normal modes (eigenvectors of the inverse Hessian matrix) overlap with the closed to open transition of CaMKII.

To this end, we formed the *transition vectors*, by subtracting the coordinates of the closed from the open structure and vice versa: $T_{closed=open-closed}$ and $T_{open=closed-open}$.

On the other hand, we performed an ANM calculation of the open and closed frames, obtaining the 3N modes (where N is the number of nodes in the elastic network, one per alpha-carbon) for each:

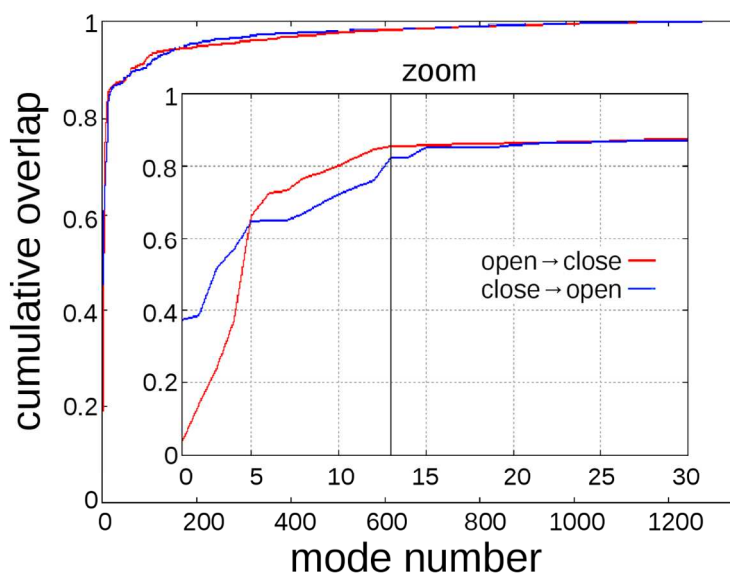
$$V_i^j = \text{mode } j \text{ of frame } i \quad (i = \text{open, closed})$$

and corresponding frequencies. Next, we calculated the cumulative overlap of the ANM modes of frame i onto the transition vector of the same frame,

$$CUM_i(j_{max}) = \sum_{j=0}^{j_{max}} V_i^j \cdot T_i$$

obtaining, thus, two CUM_i functions of j_{max} , representing the overlap of the ANM modes onto the closed to open, and open to closed transitions. In spite of the complexity of the system—a dodecamer with large electrostatic interactions, as shown later—the cumulative functions, displayed in **Fig. 2**,

1
2 show that the first 1% of the total ANM modes (13 out of a total of 1305), are enough to explain 80%
3
4 of the opening and closing of the subunit. That is, the combination of the first 13 ANM modes is
5
6 enough to span 80% of the space the system covers when going from the closed to the open
7
8 conformation. This is a result comparable to those obtained in previous studies, where it was found that
9
10 a few percent of the ANM modes is responsible for the low frequency motions of the system^{24,25}, i.e.,
11
12 those motions that determine the main structural changes of the molecule. Turning the argument
13
14 around, this fact also validates the construction and modeling of the open SUs.
15
16
17
18

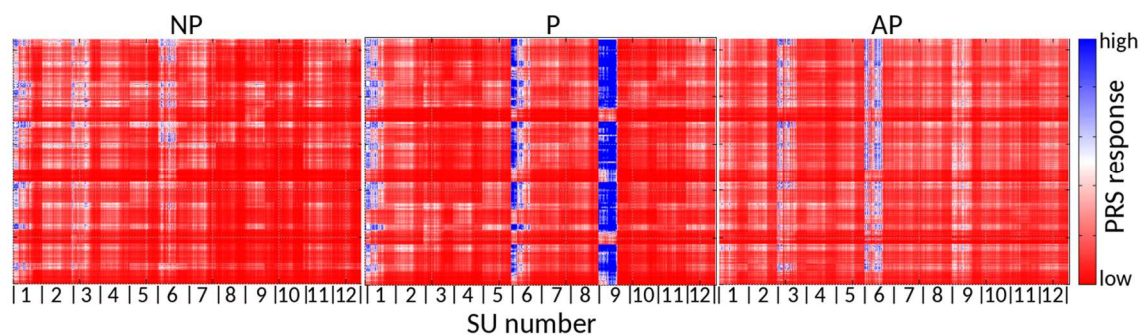


19
20
21
22
23
24
25
26
27
28
29
30
31
32
33
34
35
36
37
38
39
40
41
42
43
44
45
46
47
48
49
50
51
52
53
54
55
56
57
58
59
60
Fig. 2: Cumulative overlap of ANM modes onto open to closed (red) and closed to open (blue) structures of SU1. The first 1% of the modes, 13 out of the total 1305, explain more than 80% of the overlap. The inset is a zoomed-in image of the first 30 modes.

Phosphorylation of Subunits Changes the Influence/Sensitivity Patterns of the Molecule.

Fig. 3 shows the normalized Perturbation Response Scanning (PRS)^{26,27} maps of the NP, P and AP cases, for the cMD plus aMD simulations. The element (i,j) in the PRS matrix expresses the response of residue j to a perturbation on residue i . Thus, column j of the matrix can be interpreted as the sensitivity profile of residue j (how strongly it responds to perturbations on other residues), and row i can be seen as the influence profile of residue i (how strongly it influences other residues).

1
2 In the Figure, we can observe that the background response of the system does not change
3 much, but there are specific regions that do change significantly. In the P case, there is a strong
4 enhancement of the sensitivity of the kinases in open subunits (open kinases for short). This is seen in
5 residues 1 to 275, about 1st half in each SU, in SUs 6 and 9—especially the latter. AP also presents
6 enhancements in the open kinases corresponding to SUs 3, 6 and 9, although to a lesser extent. The fact
7 that only open kinases increase their sensitivity is not surprising, as core regions like hubs, tend to be
8 more influential, presumably due to their tight packing, while regions in the periphery—the open
9 kinases—with less structural restraints, tend to easily respond to perturbations in the core. This result
10 is, hence, suggesting that phosphorylation tends to keep the subunits open, thus making them more
11 sensitive.



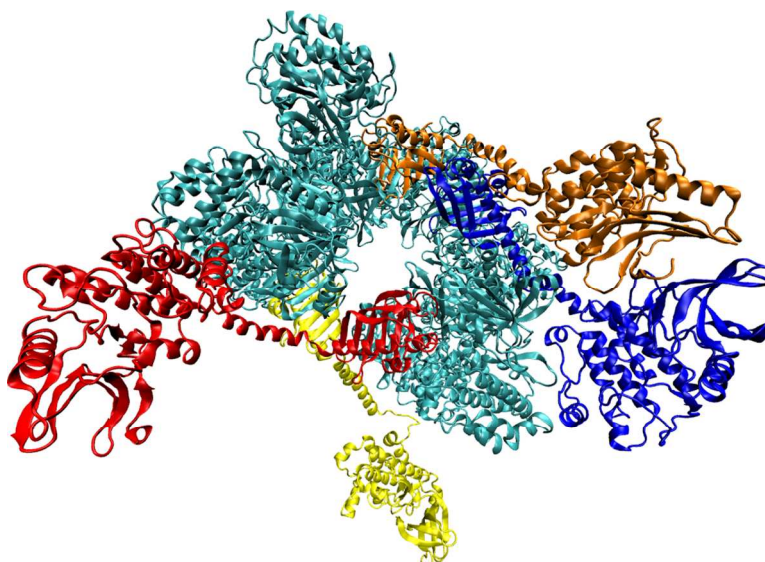
38 **Fig. 3:** PRS matrices of the NP, P and AP cases, for the aMD simulations. The kinase subdomains of
39 SU 6 and 9 show a highly increased response to perturbation in the system when T286 is
40 phosphorylated. This is diminished if T286, T305 and T306 are simultaneously phosphorylated.

41
42
43
44
45
46 Interestingly, the increase in kinase response, which can be associated to an increase in kinase
47 activity, is significantly larger in the P case. A possible explanation of this somewhat counterintuitive
48 effect will be developed in a later section. But we note here that it is in agreement with the
49 experimental results of Majeed et al¹³, where they also observe an enhanced kinase activity in the
50 double phosphorylation scenario, AP, but it is the single one, P, that shows the largest increase. (We
51 should mention that we are associating kinase activity with kinase sensitivity. The intuitive reason for
52
53
54
55
56
57
58
59
60

1
2 this—which needs to be tested further—is that, in order for a kinase to be active, it needs to sense and
3
4 react to the presence of its target; that is, it needs to be sensitive).

5
6
7 As per the mechanisms involved in the increase of sensitivity, we turn now to the observation of
8
9 the trajectories generated during the MD simulations. In the three cases, NP, P and AP, the initially
10
11 open structures do not go back to the closed conformation, but rather they lean to the side, keeping the
12
13 linker relatively stretched (see **Fig. 4**). In most cases, the linker (and a few of the first amino acids of
14
15 the kinase) of the open SU makes contact with a neighboring, closed, kinase. However, for SU6 in the
16
17 P case (orange in the Figure), due to the neighboring SU1 kinase (blue) also being open, the SU6
18
19 kinase leans on it, making full contact. This kinase-kinase interaction, with SU6 being on the outside
20
21 and influenced by the other kinase, may be responsible for the enhanced sensitivity of the SU6 kinase
22
23 (*a sensitive molecule on top of another sensitive one will become even more sensitive*).
24
25
26
27

28 The high sensitivity of SU9, in the P case (yellow in the Figure), on the other hand, has a
29
30 different explanation. This kinase stayed, during all the simulation time, away from other subunits.
31
32 Since it is free from its neighbors, it has less spatial constraints, and is thus expected to show high
33
34 sensitivity in PRS. But this may change if the simulation is continued longer, since the chance of
35
36 becoming in contact with neighbors will increase.
37
38
39



40
41
42
43
44
45
46
47
48
49
50
51
52
53
54
55
56
57
58
59 **Fig. 4:** Last frame of the accelerated MD simulation of the CaMKII dodecamer, with the closed SUs in
60

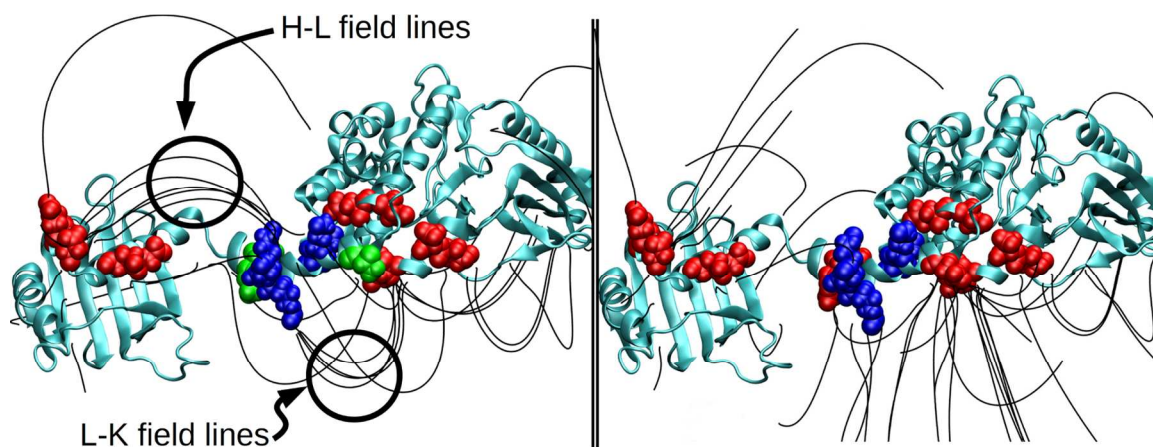
1
2 cyan and the open in different colors (SU1 blue, SU3 red, SU6 orange, SU9 yellow). The open SUs all
3
4 tend to lean to the side, and have their linkers and first part of kinase lying on the neighboring kinase.
5
6 But SU6 makes almost full contact with the SU1's linker and kinase, while SU9 maintains away from
7
8 its neighbors.
9

10
11 **Three Electrically Charged Regions in the Hub, Linker and Kinase Domains Determine**
12 **the Electrostatic Equilibrium of the Subunits, Which Is Largely Disrupted by Phosphorylation.**
13

14 We performed an electrostatic analysis of individual SUs, solving the Poisson-Boltzmann equation²⁸
15
16 for six different structures, taken from the end of the trajectories of each simulation (NP, P and AP,
17
18 both cMD and aMD). The results show three important highly charged patches, one in each domain of
19
20 the subunits, namely: E99, D100, E105, E109 and D111, in the kinase domain; K291, K292, R296,
21
22 R297, K298 and K300 in the linker; and E325, E329, D335, E337, K341, D344, E360 and D363, in the
23
24 hub domain. **Fig. 5** shows an *electrostatic pathway* of electric field lines of one of the open SUs,
25
26 connecting the three patches represented in red and blue (corresponding to negative and positive
27
28 charge, respectively). The pattern of field lines is highly organized in the NP case (left panel): high
29
30 density of lines (like the ones shown in circles) means that the end regions of those lines are strongly
31
32 attracted to each other. Thus, the left panel shows strong electrostatic attraction between H and L, and
33
34 between L and K. But that high-density pattern is largely disrupted in the AP case (right panel), and
35
36 hence the attraction between the domains is strongly weakened. This is intuitively explained by the
37
38 presence of the three residues in the linker, T286, T305 and T306, being neutral in the NP case, while
39
40 each of them acquires a negative charge in the AP case, via phosphorylation. This results in a partial
41
42 neutralization of the charged patch in L.
43
44
45
46
47
48
49
50

51
52 The aforementioned residues, E325, E329, E360 and D363, were also mentioned by Bhattacharyya et
53
54 al.²⁹, as possibly involved in the linker's binding to the hub (their numbering scheme corresponds to the
55
56 mouse sequence, as represented in the 1HKX pdb, and is slightly different to ours). As pointed out by
57
58
59
60

1
2 them, these 4 residues line the groove formed between two neighboring hubs, where the linker finds a
3
4 place to bind, facilitated by the electrostatic interaction between the negative patch in the hub and the
5
6 positive residues in the NP linker. In this way, phosphorylation of T286 breaks the electrostatic
7
8 attraction, thus reducing the linker's binding affinity to the groove.
9
10



27
28 **Fig. 5:** Subunit 1 in the open conformation. Both the hub (H), on the left, and the kinase (K), on the
29
30 right, contain negatively charged patches, shown in red, while the linker (L) presents a positively
31
32 charged patch, shown in blue. The non-phosphorylated molecule is displayed in the left panel, showing
33
34 a high density of electric field lines (shown in a circle), connecting the patches in H with L, and in L
35
36 with K. T286, T305 and T306 are shown in green when in their non-phosphorylated form. The right
37
38 panel shows the same structure, but in the phosphorylated case, where the organized structure of
39
40 electric field lines connecting H with L, and L with K, is now lost, representing a lower electrostatic
41
42 attraction between subdomains.
43
44
45

46
47
48 In order to validate these results, we repeated the analysis using representative conformations
49
50 for each simulation: for each of the six systems, the entire simulation data was divided in five root
51
52 mean square deviation based clusters, using the average linkage algorithm, in the cpptraj³⁰ analysis
53
54 program. In each case, the cluster with the greatest population was selected as representative, and
55
56 APBS was applied to it, qualitatively reproducing the above results.
57
58
59
60

We must note that, although this is a true mechanism of action observed in the simulation, the dodecamer structure complicates matters, making it possible to mix patches of one SU with patches in a neighboring one. For example, in **Fig. 4**, the H patch of SU1 (blue) interacts with the L patch of SU6 (orange). Still, the electrostatic mechanism and its alteration via phosphorylation, remains valid.

The Charged Patches in H, K and L are Highly Conserved. The strong electrostatic characteristics of the above mentioned charged patches, one in each of the subdomains, H, K and L, appear to imply their important role in the structure and/or dynamics of the system. This idea is further supported by the fact that all the residues forming those patches have identities that are well conserved in a multiple sequence alignment (MSA), composed of 111 sequences, performed using the ConSurf website³¹. In fact, if the conservation calculation³¹ considers residues with the same charge as having the same identity (a rather reasonable assumption if the charge is what gives these patches their function, as we propose), then the conservation of every residue in the K and L domains is higher than 98%. In the H subdomain, it is larger than 96%, with the exception of E325, E329 and E360, which have conservation of 90, 84 and 91%, respectively, as displayed in Table 1. The first two residues show co-evolution between them: in the MSA, every time E325 mutates, E329 also mutates (though the converse is not true). In summary, all the amino acids in the three patches show either very strong conservation or co-evolution, suggesting an important structural and/or functional role.

Table 1: Conservation of Residues that Form Each of the Three Charged Patches

	E325	E329	D335	E337	K341	D344	E360	D363
Hub	E 88%	E 76%	D 96%	E 80%	K 86%	D 98%	E 91%	D 82%
	D 02%	D 08%		D 17%	R 13%			E 15%
Linker	K291	K292	R296	R297	K298	K300		
	K 81%	K 95%	R 99%	R 99%	K 100%	K 98%		
	R 19%	R 05%				R 02%		

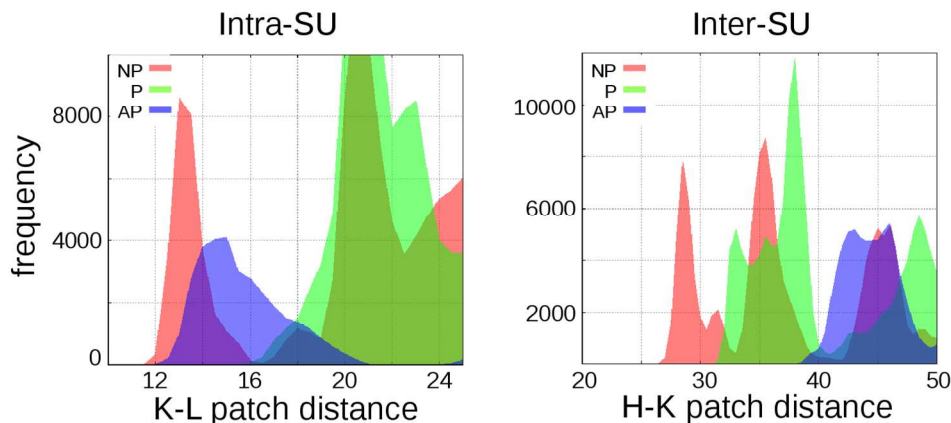
	E99	D100	E105	E109	D111
Kinase	E 96%	D 97%	E 97%	E 99%	D 96%
	D 03%	E 02%			E 03%

Sequence location and identity of residues in bold; the percentage indicates the frequency of occurrence of the given residue identity

Intra-subunit K-L, and Inter-subunit H-K, Charged Patches Tend to STICK TOGETHER in the NP Case: Autoinhibited Structures Do Not Need to be Fully Closed. From a structural point of view, the charged patches show their importance when the separation between them is analyzed. Considering all of the studied cases, a tendency toward very short separation between K and L patches belonging to the same SU, is seen in the NP case. There is only one SU in the cMD, and another one in the aMD simulation, that stay apart, around 45-50 Å (center of mass, CoM, distance). In all other cases, the shortest inter-atomic separations between patches are on the order of 10 Å, although they can get as close as 2 Å. **Fig. 6**, in its left panel, shows the distribution of CoM distances between the K and L patches, for the three cases, NP, P and AP. For short distances—the regions in which we are interested—the first peak corresponds to the NP case, expressing its tendency to shorter K-L separations. These short distances are explained by the strong electrostatic attraction between the K and L patches. Upon phosphorylation, the negative charge acquired by L serves as a partial neutralization of the previously positively charged linker which, in turn, disrupts the strong electrostatic pathway shown in **Fig. 5**, resulting in less sticky K-L patches. Hence, the K-L distances tend to increase when phosphorylation is present. We should notice the somewhat counterintuitive result that the AP case is intermediate between those two, although one would expect it to be more pronounced (larger K-L separations). But, as previously mentioned in reference to the PRS maps, this result appears to be in agreement with Majeed et al¹³, where they observe a significantly enhanced kinase activity in the P case, but a lower enhancement in the AP case.

This difference in separation between subdomains is not observed in relation to the L and H patches, presumably due to the rigid nature of the hub—which constitutes the core of the CaMKII

1
2 system—as opposed to the very flexible linker. The kinase, being on the periphery of the system, is less
3
4 constrained, and is able to follow the linker in its high entropy trajectory, thus their charged patches
5
6 staying in close proximity.
7
8



9
10
11
12
13
14
15
16
17
18
19
20
21
22
23
24
25 **Fig. 6:** Normalized frequency distributions of the center of mass distances of charged patches K and L
26 of the same SU (left panel), and H and K of neighboring SUs (right panel). The NP case (red) has
27 larger contributions for short separations, followed by P (green) and AP (blue), indicating the strong
28 effect of phosphorylation in these distributions.
29
30
31
32
33
34
35

36 On the other hand, since a subunit can become very long when in the open conformation, up to
37 about 130 Å, it is not uncommon to find one stretching over another neighboring SU (as shown in **Fig.**
38 **4**). In such cases, interactions between charged patches of neighboring SUs are important; moreover,
39 this seems to be the norm rather than the exception, as it is observed in virtually all of the SUs; their
40 initially open linker-kinase tends to stretch to a side, more than to return to their closed conformation
41 (this was not observed only in one SU of the P case, where the kinase lingered above of its
42 corresponding hub). In particular, if we consider the separation between H and K patches of
43 neighboring SUs (**Fig. 6**, right panel), we observe that they are found closest in the NP case. Again, the
44 explanation is the stronger H-L-K attraction when the system is not partially neutralized by
45 phosphorylation. It is not really important if the interaction is intra- or inter-subunit, as the behavior
46
47
48
49
50
51
52
53
54
55
56
57
58
59
60

1
2 appears to be determined only by the net charge of the involved patches, not by their belonging.
3

4 The minimum H-K CoM distances are about 26Å for NP, 31Å for P and 38Å for AP. These are
5 relatively small differences, especially when considering the length of the open SU; visually, the
6 phosphorylated and non-phosphorylated conformations look alike. This is suggesting an alternative to
7 the usual interpretation of the inactive state, where the inhibited SU is thought as being fully closed (H
8 and K of the same SU bound to each other). In view of the right panel of Figure 6, we propose that an
9 inactive state could also be related to a conformation where the subunit is open, but its kinase domain is
10 attached to a neighboring hub, with separations between them of ~ 26Å. And the active state could be
11 associated with the kinase separated only a few more angstroms from that value (~31Å for P, 38Å for
12 AP). The former states resemble the *activation-competent conformations* observed by Myers et al³²
13 using single particle electron microscopy; that is, conformers where K domains are not attached to their
14 corresponding H, while not being in the active state.
15
16
17
18
19
20
21
22
23
24
25
26
27
28
29

30 **Phosphorylation of T305/T306 May or May Not Enhance the Effect of Phosphorylating**
31 **T286.** As previously noted in relation to the PRS maps and the K-H distances, the change in behavior
32 observed when going from the NP to the P case is compatible with the fact that the attraction of H-L-K
33 is diminished upon phosphorylation. Thus, K can get a few more angstroms away from H, becoming
34 more detached, hence, more sensitive and with more freedom in its function as a kinase to *search* for a
35 residue suitable for phosphorylation.
36
37
38
39
40
41
42
43
44

45 When also phosphorylating residues T305 and T306 we would, in principle, expect the above
46 mechanism to be enhanced, but that is not what we have found (in agreement with Majeed et al¹³), as
47 previously analyzed and shown in **Fig. 3** and **Fig. 6**. Does MD provide an explanation for this
48 unintuitive fact? We believe it does.
49
50
51
52
53

54 **Fig. 7** shows a detailed view of the positional relation between an open SU and a neighboring
55 one, in the different phosphorylation scenarios. There, the distance between the brown kinase and blue
56 hub does not seem to greatly vary (compatible with **Fig. 6**). Then, how can we explain the unexpected
57
58
59
60

1
2 behavior of AP? Comparison of each image with its corresponding inset, allows to appreciate the
3 separation between phosphorylation sites T286 vs T305-306. We observe that their separation is greatly
4 separation between phosphorylation sites T286 vs T305-306. We observe that their separation is greatly
5 increased in the AP case (see also first peak of each case in last panel). The reason for this is simply,
6 and once again, the electrostatic repulsion between the sites—fully phosphorylated in AP—while there
7 was no repulsion at all in the NP and P cases (since NP has the 3 sites neutral, and P only has T286
8 charged). If this distance was fixed, we would have a reason to expect the AP case to show an
9 enhancement of the effects in P; but since the distance doubles in the AP case, we don't have a reason
10 to expect such enhancement. And what we actually see is the opposite, a sort of dampening of the
11 effect, where the AP sensitivity (Fig. 3) and the K-L distance (Fig. 6, left) are intermediate between NP
12 and P.
13
14
15
16
17
18
19
20
21
22
23
24
25
26
27
28
29
30
31
32
33
34
35
36
37
38
39
40
41
42
43
44
45
46
47
48
49
50
51
52
53
54
55
56
57
58
59
60

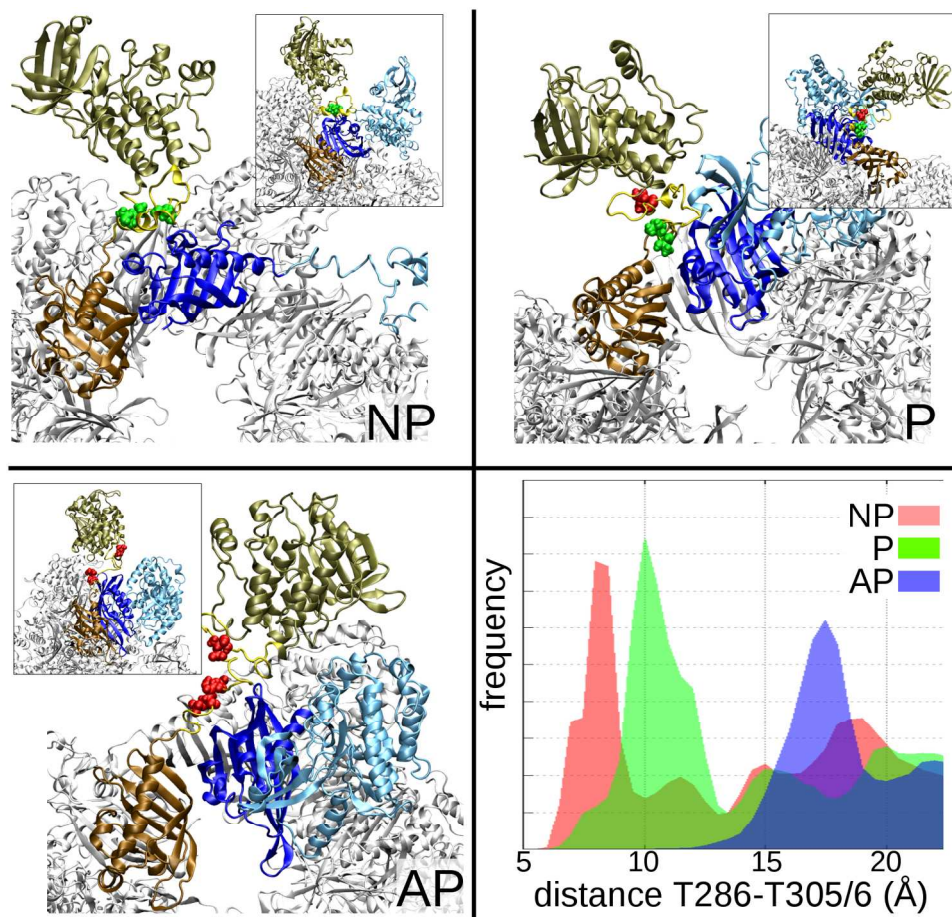


Fig. 7: Detailed view of the positional relation between an open SU and a neighboring one, in the NP,

1
2 P and AP cases. Two subunits are shown, in brown and blue shades respectively, along with the three
3 phosphorylation sites, T286, 305 and 306, in red or green spheres, depending on whether they are, or
4 are not, phosphorylated. Each panel contains an inset, with a rotated view of the same image. The AP
5 case distinguishes from the other in that the T286 vs T305/306 distance is greatly increased (as a
6 consequence of electrostatic repulsion). Also shown is a panel with the histogram of distances between
7 those sites.
8
9
10
11
12
13
14
15

16
17 **Hubs in Closed SUs are More Stable Than Open Ones.** Fig. 8 shows, in its left panel, the
18 total energy of each of the twelve hub subdomains of the dodecamer. Closed hubs tend to be lower in
19 energy when compared to open ones, average $\Delta E(\text{closed-open}) = -95 \pm 5$ kcal/mol. In addition, within
20 open SUs, it is observed that the phosphorylated cases have a higher average energy: -1590, -1578, -
21 1551 kcal/mol, for the NP, P and AP cases, respectively. There are studies showing that activation of
22 CaMKII negatively affects the stability of the core, leading to an eventual release of a subunit^{15,29}. Our
23 results hint at this fact, that open conformations, particularly phosphorylated ones, tend to destabilize
24 the core, favoring the release of the subunit from the dodecamer.
25
26
27
28
29
30
31
32
33
34
35

36 This point should be studied further, as we are ignoring entropic effects (which one should in principle
37 include since what determines the stability of the system is its free energy, not its energy). These
38 entropic effects will, presumably, reduce the separation between the open and closed subunits
39 mentioned in the previous paragraph: the entropy of the hub in the closed case is, arguably, going to be
40 lower than that of the open case, since the subdomain is trapped between the neighboring hubs and the
41 closed kinase, having less freedom to move; this would decrease its entropy and increase its free
42 energy. Nevertheless, the large energetic difference of about 95 kcal/mol, between the average open
43 and closed hubs, seems too large to be overcome by entropic effects, and thus, the closed form should
44 remain more stable.
45
46
47
48
49
50
51
52
53
54
55
56
57
58
59
60

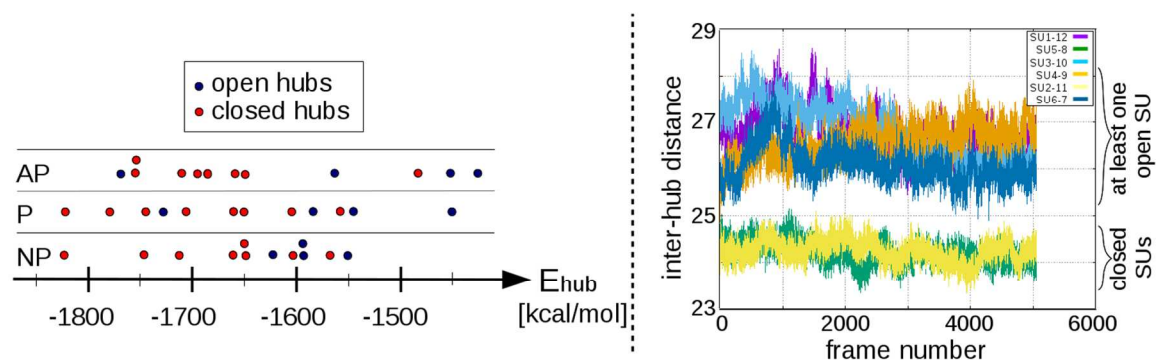


Fig. 8: Left panel) Self-energy of the hubs of each of the 12 subunits of the NP, P and AP cases. The closed conformations (red points) tend to have less energy than the open ones (blue points), suggesting a higher stability. Average open/closed hub energy = $-1573 / -1668$ kcal/mol $\rightarrow \Delta(\text{closed} \rightarrow \text{open}) = -95 \pm 5$ kcal/mol. Right panel) inter-hub distance for vertical dimers of hubs (first neighbors in different rings). The two cases where the two hubs correspond to closed SUs show a significantly lower separation (picture shows the NP-cMD case, but is representative of all cases).

We have also observed that the inter-hub (first neighbors, in different rings) separation is significantly increased when one or the two hubs belongs to open SUs. This is represented in the right panel of **Fig. 8**, where there is a very clear separation between cases with the two hubs corresponding to closed SUs (green and yellow lines, at the bottom) and other cases. The average change in separation is 2.3 ± 0.5 Å. This is in correspondence with the previous energetic result, since a closer, tighter packing of the hubs is associated with a lower energy and, hence, increased stability. It should be noted that there is no significant difference in separations between the NP, P and AP cases.

CONCLUSIONS

In summary, with the goal of studying the closed and open conformations of the subunits, and the effect of phosphorylation, we prepared six systems of CaMKII in dodecameric form, with eight closed and four open SUs. Two systems were wild type, not phosphorylated, two had a phosphorylated T286,

1
2 and two had phosphorylation in T286, T305 and T306. We chose those specific residues since they
3
4 were mentioned in the literature as responsible for the trigger of signals related to activation of
5
6 CaMKII. One of the systems of each of the mentioned states was used to perform conventional MD,
7
8 while the other was the starting point of accelerated MD, which is capable of accelerating the
9
10 dynamics, increasing the effective coverage of the conformational space by the simulation. In this way,
11
12 we covered the possibility of not doing enough cMD to see important effects.
13
14

15
16 The main finding of the present study is the determination of three specific regions of the hub,
17
18 linker and kinase of every subunit, characterized by a significant electric charge. These charged patches
19
20 are shown to play an important role in the interactions between the subdomains, via a K-L-H
21
22 electrostatic pathway formed by them, as shown in **Fig. 5**. In particular, the NP case shows a strong
23
24 interaction between H and L, and between L and K. This is partially lost when T286 or T286, T305 and
25
26 T306 acquire a phosphate group, as their negative charge tends to neutralize the originally positive
27
28 charge of the L patch, effectively weakening the interaction pathway.
29
30
31

32
33 The relevance of these charged regions is further supported by a conservation analysis of the
34
35 identity of the amino acids forming the three patches. Table 1 shows the high conservation of each of
36
37 those residues. But when the analysis is done taking into account not the specific amino acid identity,
38
39 but rather their net electric charge, the conservation scores become much higher, in most cases above
40
41 97%. And the two residues that have the lowest conservation show a strong co-evolution between
42
43 them. The existence of these patterns highlights the evolutionary importance of those regions being
44
45 charged, and strongly suggests they are fundamental for the function of the molecule.
46
47
48

49
50 From a structural point of view, it is frequently speculated that the separation between K and H
51
52 of the same SUs greatly increases upon activation and goes back to its original conformation when
53
54 deactivated (not phosphorylated). This is not what we have observed: once the SUs are open, they don't
55
56 go back to the initial closed conformations, with K fully attached to H (although we don't discard this
57
58 possibility, as it may just be out of our simulation time scale). Rather, K and H stay apart, and their
59
60

1
2 CoM separation is a bit larger for the phosphorylated cases. The distance between the first peaks of the
3
4 NP and AP cases in the left panel of **Fig. 6** is 2Å. This means that the conformational changes
5
6 occurring as a cause of phosphorylation are subtler than usually thought. If we look at the separation
7
8 between patches of neighboring SUs, the situation is similar, in that the distance H-K is significantly
9
10 lower for the NP case, followed by the P, and lastly AP case (right panel of **Fig. 6**). Again, this
11
12 behavior can be rationalized by the stronger electric charge of the L patch, in the NP case, that acts as a
13
14 *glue* between H and K. As phosphorylation neutralizes the charge of L, the glue weakens, and the
15
16 repulsion between the like charges in H and K starts to dominate, leading to an increased separation.
17
18
19
20
21 This image is consistent with the *activation-competent conformations* observed by Myers et al³².
22

23
24 The overall picture arising from this study is that the three mentioned charged patches are key
25
26 in enabling and disabling the interactions between the SUs' subdomains, both in an inter- and intra-SU
27
28 fashion. When in the NP state, the interactions are fully operational, and there is a strong attraction that
29
30 tends to keep the different domains close to each other. Upon phosphorylation, the charge of the L
31
32 patch is partially neutralized, leading to a breakage of that attractive force, so the kinase domain
33
34 becomes looser. This leads to a few angstroms increase of the intra-SU K-L and inter-SU H-K
35
36 separations. In turn, the hub, being now partially unbound from one side (the kinase side), experiences
37
38 an increase in its self-energy, becoming less stable; this is particularly true for hubs in phosphorylated
39
40 SUs, since their energy is larger than the one of those on non-phosphorylated SUs (**Fig. 8**). This, maybe
41
42 coupled to a similar event on a neighboring subunit, may lead to the destabilization of the whole
43
44 subunit, ending in a release of a monomer of CaMKII, or perhaps a dimer, as noted in other studies^{15,29}.
45
46
47
48
49
50

51 **Acknowledgement**

52
53
54
55 We thank Prof. Ivet Bahar for helpful discussions and for her support. We also acknowledge Agencia
56
57 Nacional de Promocion Cientifica y Tecnologica, for their grants PICT-2015-1706 (E.K.A.) and PICT-
58
59
60

1
2 2015-3832 (I.J.G.).
3
4
5
6

7 REFERENCES

10 1- Anderson, M. Calmodulin kinase signaling in heart: an intriguing candidate target for therapy of
11 myocardial dysfunction and arrhythmias. *Pharmacol Ther.* **2005**, *106*, 39-55.
12

15 2- Fährmann, M.; Kaufhold, M. A. Functional partitioning of epithelial protein kinase CaMKII in
16 signal transduction. *Biochim Biophys Acta* **2006**, *1763*, 101-109.
17

20 3- Skelding K. A.; Rostas J. A.; Verrills N. M. Controlling the cell cycle: the role of
21 calcium/calmodulin-stimulated protein kinases I and II. *Cell Cycle* **2011**, *10*, 631-639.
22

25 4- Lin M. Y.; Zal T.; Ch'en I. L.; Gascoigne N. R. J.; Hedrick S. M. A pivotal role for the
26 multifunctional calcium/calmodulin-dependent protein kinase II in T cells: From activation to
27 unresponsiveness. *J Immunol.* **2005**, *174*, 5583-5592.
28
29

32 5- Lisman, J. Holoenzymes: Refreshing memories. *eLife* **2014**, *3*, e02041
33

36 6- Tombes, R. M.; Faison, M. O.; Turbeville J. M. Organization and evolution of multifunctional
37 Ca(2+)/CaMdependent protein kinase genes. *Gene* **2003**, *322*, 17-31.
38

41 7- Bayer K. U.; De Koninck, P.; Schulman H. Alternative splicing modulates the frequency-dependent
42 response of CaMKII to Ca²⁺ oscillations. *EMBO J* **2002**, *21*, 3590-3597.
43

46 8- Wang, P.; Wu, Y-L.; Zhou, T-H.; Sun, Y.; Pei, G. Identification of alternative splicing variants of
47 the β subunit of human Ca²⁺/calmodulin-dependent protein kinase II with different activities. *FEBS*
48 *Letters* **2000**, *475*, 110.
49

52 9- De Koninck, P; Schulman, H. Sensitivity of CaM kinase II to the frequency Ca²⁺ oscillations.
53 *Science* **1998**, *279*, 227-230.
54
55
56
57
58
59
60

1
2 10- Giese, K. P.; Fedorov, N. B.; Filipkowski, R. K.; Silva, A. J. Autophosphorylation at Thr286 of the
3
4 alpha calcium-calmodulin kinase II in LTP and learning. *Science* **1998**, *279*, 870-873.
5

6
7 11- Hanson, P. I.; Schulman, H. Inhibitory autophosphorylation of multifunctional Ca²⁺/calmodulin-
8
9 dependent protein kinase analyzed by site-directed mutagenesis. *J. Biol. Chem.* **1992**, *267*, 17216-
10
11 17224.
12

13
14 12- Colbran, R. J. Inactivation of Ca²⁺/calmodulin-dependent protein kinase II by basal
15
16 autophosphorylation. *J Biol Chem.* **1993**, *268*, 7163-7170.
17

18
19 13- Majeed, A. B. B.; Pearsall, E.; Carpenter, H.; Brzozowski, J. S.; Dickson, P. W.; Rostas, J. A. P.;
20
21 Skelding, K. A. CaMKII kinase activity, targeting and control of cellular functions: Effect of single and
22
23 double phosphorylation of CaMKII α , *Calcium Signaling* **2014**,*1*, 36-51.
24
25

26
27 14- Elgersma, Y.; Fedorov, N. B.; Ikonen, S; Choi, E. S.; Elgersma, M.; Carvalho, O. M.; Silva, A. J.
28
29 Inhibitory autophosphorylation of CaMKII controls PSD association, plasticity, and learning. *Neuron*
30
31 **2002**, *36*, 493-505.
32
33

34
35 15- Stratton, M.; Lee, I-H.; Bhattacharyya, M.; Christensen, S. M.; Chao, L. H.; Schulman, H.; Groves,
36
37 J. T.; Kuriyan, J. Activation-triggered subunit exchange between camkii holoenzymes facilitates the
38
39 spread of kinase activity. *eLife* **2013**, *3*, e01610.
40
41

42
43 16- Chao, L. H.; Stratton, M. M.; Lee, I-H.; Rosenberg, O. S.; Levitz, J.; Mandell, D. J.; Kortemme, T.;
44
45 Groves, J. T; Schulman, H.; Kuriyan, J. A Mechanism for tunable autoinhibition in the structure of a
46
47 human Ca²⁺ /calmodulin-dependent Kinase II holoenzyme. *Cell* **2011**, *146*, 732-745.
48
49

50
51 17- Rellos, P.; Pike, A. C. W.; Niesen, F. H.; Salah, E.; Lee, W. H.; von Delft, F.; Knapp, S. Structure
52
53 of the CaMKII δ /Calmodulin complex reveals the molecular mechanism of CaMKII kinase
54
55 activation. *PLoS Biol.* **2010**, *8*, 426.
56
57

58 18- Jorgensen, W. L.; Chandrasekhar, J.; Madura, J. D.; Impey, R. W.; Klein, M. L. Comparison of
59
60

- 1
2 simple potential functions for simulating liquid water. *J. Chem. Phys.* **1983**, *79*, 926-935.
3
4
5 19- Case, D. A.; Berryman, J. T.; Betz, R. M.; Cerutti, D. S.; Cheatham III, T. E.; Darden, T. A.; Duke,
6
7 R. E.; Giese, T. J.; Gohlke, H.; Goetz, A. W.; et al. *AMBER 2015*, University of California, San
8
9 Francisco, 2015.
10
11
12 20- Homeyer, N.; Horn, A. H. C.; Lanig, H.; Sticht, H. AMBER force field parameters for
13
14 phosphorylated amino acids in different protonation states: Phosphoserine, phosphothreonine,
15
16 phosphotyrosine and phosphohistidine. *J. Mol. Model.* **2006**, *12*, 281-289.
17
18
19
20 21- Bryce, R. A. Manchester Pharmacy School, University of Manchester, Oxford Road, Manchester
21
22 M13 9PL, UK. <http://sites.pharmacy.manchester.ac.uk/bryce/amber>
23
24
25 22- Hamelberg, D.; Mongan, J.; McCammon, J. A. Accelerated molecular dynamics: A promising and
26
27 efficient simulation method for biomolecules. *J. Chem. Phys.* **2004**, *120*, 11919–11929.,
28
29
30
31 23- Atilgan, A. R.; Durrell, S. R.; Jernigan, R. L.; Demirel, M. C.; Keskin, O.; Bahar, I. Anisotropy of
32
33 fluctuation dynamics of proteins with an elastic network model. *Biophys. J.* **2001**, *80*, 505-515.
34
35
36 24- Bahar, I.; Lezon, T. R.; Bakan, A.; Shrivastava, I. H. Normal mode analysis of biomolecular
37
38 structures: Functional mechanisms of membrane proteins. *Chem. Rev.* **2010**, *110*, 1463–1497.
39
40
41 25- Das, A.; Gur, M.; Cheng, M. H.; Jo, S.; Bahar, I.; Roux, B. Exploring the conformational
42
43 transitions of biomolecular systems using a simple two-state anisotropic network model. *PLoS Comput.*
44
45 *Biol.* **2014**, *10*, e1003521.
46
47
48
49 26- Atilgan, C.; Atilgan, A. R. Perturbation-response scanning reveals ligand entry-exit mechanisms of
50
51 ferric binding protein. *PLoS Comput. Biol.* **2009**, *5*, e1000544.
52
53
54 27- General, I. J.; Liu, Y.; Blackburn, M.; Mao, W.; Gierasch, L.; Bahar, I. ATPase subdomain IA is a
55
56 mediator of interdomain allostery in Hsp70 molecular chaperones. *PLoS Comput. Biol.* **2014**, *10*,
57
58 e1003624.
59
60

1
2 28- Dolinsky, T. J.; Nielsen, J. E.; McCammon, J. A., Baker, N. A. PDB2PQR: An automated pipeline
3
4 for the setup, execution, and analysis of Poisson-Boltzmann electrostatics calculations. *Nucleic Acids*
5
6 *Res.* **2004**, *32*, W665-W667.
7

8
9
10 29- Bhattacharyya, M.; Stratton, M. M.; Going, C. C.; McSpadden, E. D.; Huang, Y.; Susa, A. C.;
11
12 Elleman, A.; Cao, Y. M.; Pappireddi, N.; Burkhardt, P.; et al. Molecular mechanism of activation-
13
14 triggered subunit exchange in Ca(2+)/calmodulin-dependent protein kinase II. *eLife* **2016**, *5*, e13405.
15

16
17 30- Roe, D. R.; Cheatham, T. E., III. PTRAJ and CPPTRAJ: Software for processing and analysis of
18
19 molecular dynamics trajectory data. *J. Chem. Theory Comput.* **2013**, *9*, 3084-3095.
20

21
22 31- Celniker, G.; Nimrod, G.; Ashkenazy, H.; Glaser, F.; Martz, E.; Mayrose, I.; Pupko, T.; Ben-Tal,
23
24 N. ConSurf: Using evolutionary data to raise testable hypotheses about protein function. *Isr. J. Chem.*
25
26 **2013**, *53*, 199–206.
27

28
29
30 32- Myers, J. B.; Zaegel, V.; Coultrap, S. J.; Miller, A. P.; Bayer, K. U.; Reichow, S. L. The CaMKII
31
32 holoenzyme structure in activation-competent conformations. *Nat Commun.* **2017**, *8*: 15742.
33
34
35
36
37
38
39
40
41
42
43
44
45
46
47
48
49
50
51
52
53
54
55
56
57
58
59
60

TOC IMAGE

